Prevention of Murine Antiphospholipid Syndrome by BAFF Blockade

Philip Kahn[1], **Meera Ramanujam**[1], **Ramalingam Bethunaickan**[1], **Weiqing Huang**[1], **Haiou Tao**[1], **Michael P. Madaio**[2], **Stephen M. Factor**[3], and **Anne Davidson**[1]

Abstract

Objective—This study was undertaken to determine whether BAFF blockade can be used to prevent or treat antiphospholipid syndrome in a mouse model.

Methods—Eight- and 12-week-old $(NZW \times BXSB)F_1$ mice were treated with BAFF-R-Ig or TACI-Ig alone or in addition to a short course of CTLA-4Ig. Mice were monitored for thrombocytopenia and proteinuria. Sera were tested for anticardiolipin antibodies (aCL), BAFF levels, and levels of soluble vascular cell adhesion molecule and E-selectin. Mice were killed at 17, 22, or 32 weeks of age, and kidneys and hearts were subjected to histologic examination. Spleen cells were phenotyped and enzyme-linked immunospot assays for auto-antibody-producing B cells were performed.

Results—Both BAFF-R-Ig and TACI-Ig prevented disease onset and significantly prolonged survival. Treated mice had significantly smaller spleens than controls, with fewer B cells and fewer activated and memory T cells. BAFF blockade did not prevent the development of aCL, and there was only a modest delay in the development of thrombocytopenia. However, treated mice had significantly less nephritis and myocardial infarcts than did controls.

Conclusion—Our findings suggest that aCL are generated in the germinal center, which is relatively independent of BAFF. Effector function of antiplatelet antibodies was only modestly affected by BAFF blockade. In contrast, myocardial infarctions were prevented, suggesting that triggering of thromboses requires both autoantibodies and mediators of inflammation. Similarly, renal damage requires both immune complexes and effector cells. The dissociation between autoantibody production and inflammation that may occur with B cell–depleting therapies underscores the role of B cells as effector cells in the autoimmune response.

Address correspondence and reprint requests to Anne Davidson, MBBS, Investigator, Feinstein Institute for Medical Research, 350 Community Drive, Manhasset, NY 11030. E-mail: adavidson1@nshs.edu.
[1]Philip Kahn, MD (current address: Morgan Stanley Children's Hospital of New York–Columbia Medical Center, New York, New York), Meera Ramanujam, PhD, Ramalingam Bethunaickan, PhD, Weiqing Huang, MD, Haiou Tao, BSc, Anne Davidson, MBBS: Feinstein Institute for Medical Research, Manhasset, New York
[2]Michael P. Madaio, MD: Temple University, Philadelphia, Pennsylvania
[3]Stephen M. Factor, MD: Albert Einstein College of Medicine, Bronx, New York.

Drs. Kahn and Ramanujam contributed equally to this work.

Antiphospholipid syndrome (APS) is a disease manifested by dysregulated clotting in both the arterial and venous systems and is caused by antibodies to phospholipids and their binding protein β_2-glycoprotein I (1). The autoantibodies that cause APS are unresponsive to conventional immunosuppression, which suggests that they may be derived from a long-lived B cell subset.

The (NZW × BXSB)F$_1$ mouse is a murine model of spontaneous APS. The male offspring of this cross produce anticardiolipin antibodies (aCL) and anti-RNP antibodies by 12 weeks of age, and subsequently develop immune-mediated thrombocytopenia, inflammatory glomerulonephritis (GN), and a thrombotic vasculopathy of the small coronary arteries, which leads to myocardial infarcts, myocardial fibrosis, and a dilated cardiomyopathy. Full-thickness infarcts affecting the right ventricle are seen in the late stages of disease (2,3).

APS in (NZW × BXSB)F$_1$ mice is dependent upon both B and T cells and development of autoantibodies. Thrombocytopenia and nephritis are completely prevented by CD4 T cell depletion before 6–8 weeks of age (4). We have shown that the B7/CD28 antagonist CTLA-4Ig blocks class switching of antiphospholipid antibodies (aPL) to the IgG isotype and prevents both nephritis and coronary thromboses when given at 8 weeks of age, before the emergence of autoantibodies (5). However, administration of CTLA-4Ig at 12 weeks of age, after the development of autoantibodies, no longer prevents the disease (5). These findings indicate that the pathogenetic B cells in (NZW × BXSB)F$_1$ mice arise in a CD4 T cell– and CD28-dependent manner but that B7/CD28 interactions are not required for disease perpetuation.

Male (NZW × BXSB)F$_1$ mice bear the *Yaa* gene, a reduplicated segment of the Y chromosome containing the genes for Toll-like receptor 7 (TLR-7) and TLR-8, intracellular single-stranded RNA–sensing TLRs expressed by plasmacytoid dendritic cells (DCs) and B cells (6). Activation of TLR-7 in plasmacytoid DCs induces the release of type I interferons that stimulate myeloid DCs to release BAFF, a tumor necrosis factor (TNF)–like cytokine that is crucial for B cell survival (for review, see refs. 7 and 8). BAFF expands the B cell compartment, leading to increased production of immune complexes that can further activate TLRs (9). We therefore hypothesized that BAFF blockade may be a successful therapeutic approach for APS, even in the later stages of disease.

BAFF and its homologous molecule APRIL interact with 3 different BAFF receptors on B cells: TACI, BAFF-R, and BCMA. These interactions can be blocked by soluble Ig fusion proteins of the BAFF receptors TACI or BAFF-R. BAFF-R-Ig selectively blocks only BAFF, whereas TACI-Ig blocks both BAFF and APRIL (for review, see ref. 10). We found that blockade of BAFF alone is sufficient to prevent disease both in the early and late initiation stages.

MATERIALS AND METHODS

Mice

Female NZW and male BXSB mice were purchased from The Jackson Laboratory (Bar Harbor, ME) and bred in our institution. Male (NZW × BXSB)F1 progeny were divided into groups and treated with either a single intravenous injection of adenovirus expressing TACI-Ig (AdTACI-Ig) (11) at 8 weeks of age (n = 14 mice), a single intravenous injection of adenovirus expressing BAFF-R-Ig (AdBAFF-R-Ig) (12) at 8 weeks of age (n = 31 mice) or 12 weeks of age (n = 23 mice), a single intravenous injection of adenovirus expressing CTLA-4Ig (AdCTLA-4Ig) (13) at 12 weeks of age (n = 14 mice), a combination of an injection of AdBAFF-R-Ig at 8 weeks of age and 6 100-μg doses of CTLA-4Ig given intraperitoneally over a 2-week period (n = 10 mice), or a single injection of AdLacZ at 8 weeks of age (n = 15 mice).

All viruses were given at doses of 1×10^{11} particles per mouse. A control group (n = 100 mice) received no treatment.

Mice were tested for proteinuria every 2 weeks (Multistick; Fisher Scientific, Pittsburg, PA) and bled periodically for serologic analysis. Platelets were counted with a Coulter counter (Beckman Coulter, Fullerton, CA) at 8, 17, and 22 weeks of age. Mice in the AdBAFF-R-Ig–treated and control groups (6–8 mice per group) were killed at each of the following time points: at 17 weeks, when maximal autoantibody production occurred, at 22 weeks, when 50% of the controls had developed proteinuria, and at 32 weeks, when >70% of the control mice were dead. Moribund mice were killed, and organs were processed for histologic analysis.

Antibodies to cardiolipin and Sm/RNP

Serial serum samples were available from 7 mice treated with AdBAFF-R-Ig at 8 weeks, 7 mice treated with AdBAFF-R-Ig at 12 weeks, and 8 untreated controls. Antibodies to Sm/RNP and cardiolipin were measured by enzyme-linked immunosorbent assay (ELISA). Sm/RNP (Arotec Diagnostics, Wellington, New Zealand) was coated onto Falcon plates (BD Labware, Franklin Lakes, NJ) at 1 μg/ml in phosphate buffered saline (PBS). The assay was then performed according to the recommendations of the manufacturer (Arotec Diagnostics). To measure anticardiolipin titers, Immulon 2HB plates (Fisher Scientific) were coated with 75 μg/ml cardiolipin (Sigma, St. Louis, MO) in ethanol and allowed to dry. Plates were blocked with 5% fetal calf serum (FCS)/3% bovine serum albumin (BSA) in PBS for 90 minutes at room temperature and then incubated for 2 hours with serum diluted 1:500 in PBS/1% BSA. FCS in the blocking solution is a source of β2-glycoprotein I. Plates were developed with alkaline phosphatase–conjugated goat anti-mouse IgG or IgM (Southern Biotechnology, Birmingham, AL) diluted 1:1,000 in PBS/1% BSA, followed by BCIP substrate (Sigma). A high-titer positive serum was run in serial dilution on each plate as a quantitation control. To determine relative affinity of the IgG antibodies, sera from 17-week-old mice were normalized to the concentration required for 80% maximal binding to the plates. This concentration of serum (250 μl) was then preincubated overnight at 4°C with 25 μl of buffer alone or buffer containing increasing amounts of soluble cardiolipin, and the mixture was then subjected to ELISA, as described above. Percentage inhibition was calculated using a standard binding curve derived from a high-titer serum.

Enzyme-linked immunospot (ELISpot) assay

ELI-Spot assay for total IgM- and IgG-secreting cells and IgM and IgG anticardiolipin–secreting cells was performed on spleen and bone marrow cells as previously described (5), using 5–8 mice per group.

Flow cytometry

Spleens were analyzed for B and T cell markers using antibodies to CD4 (Caltag, Burlingame, CA), CD8 (Caltag), and CD19. Spleen DCs were identified using phycoerythrin-conjugated anti-CD11b and fluorescein isothiocyanate–conjugated anti-CD11c. B cell subsets were classified as follows: mature follicular (CD19+IgM+IgD+), marginal zone (CD19 +CD21^{high}CD23^{low}), class-switched (CD19+IgM^{low}IgD^{low}), or immature (CD19 +IgM^{high}IgD^{low}) B cells. CD4+ T cells were classified as naive (CD62L^{high} CD44^{low}) or memory (CD62L^{low}CD44^{high}) T cells. Activated T and B cells were defined as CD69+ cells. Unless otherwise stated, all antibodies were obtained from BD PharMingen (San Diego, CA).

Histologic analysis of mouse kidneys and hearts

Mice were anesthetized, and their hearts were perfused with sterile saline to remove red blood cells. Hematoxylin and eosin (H&E)–stained sections of the kidneys were examined and scored

on a scale of 1–4 for glomerular damage and interstitial inflammation, as previously described (14). Hearts were sectioned into 4 slices, and each slice was examined for ischemia, necrosis, scarring, and inflammation as previously described (5). Myocardial damage was scored on a scale of 1–4, based on the degree of inflammation and fibrosis, where 1 = a single area of necrosis, 2 = several areas of necrosis and fibrosis, 3 = extensive focal areas of necrosis and fibrosis, and 4 = full-thickness myocardial infarct (5). Histologic analyses were performed by observers who were blinded with regard to treatment group.

Immunohistochemical analysis of kidneys was performed using antibodies for IgG (Southern Biotechnology), CD4, B220, CD11c, and F4/80. Slides were counterstained with 4′,6-diamidino-2-phenylindole (Invitrogen, Carlsbad, CA), and images were captured using a digital CCD camera system connected to a Zeiss microscope (Zeiss, Thornwood, NY).

Real-time polymerase chain reaction (PCR) analysis of kidneys

One kidney from each perfused mouse was used to prepare total RNA, which was subjected to real-time PCR analysis exactly as previously described (15), using primers for vascular cell adhesion molecule (VCAM), intercellular adhesion molecule (ICAM), E-selectin, and P-selectin. Normalized expression data were $\log^2$-transformed and scaled to the expression value for a single 8-week-old mouse, which was assigned an arbitrary value of 1.

Quantitation of serum levels of BAFF, VCAM, and E-selectin

Serum from treated and untreated mice was harvested and immediately frozen at −80°C until used. BAFF, VCAM, and E-selectin levels were measured using commercial kits according to the recommendations of the manufacturer (R&D Systems, Minneapolis, MN).

Statistical analysis

Proteinuria and survival data were analyzed using Kaplan-Meier curves and the log rank test. Comparisons were performed using Wilcoxon's rank sum test. Only significant P values are shown.

RESULTS

Frozen sera from untreated 10-week-old mice (n = 5), 15–17-week-old mice (n = 13), and mice older than 20 weeks (n = 8) were tested for soluble BAFF levels by ELISA. BAFF levels were normal in 10-week-old mice (mean ± SD 16.8 ± 11.2 ng/ml) but were increased in mice at 15–17 weeks of age (mean ± SD 38.6 ± 19.6 ng/ml; $P < 0.03$) and were further increased in older mice (82.5 ± 56.2 ng/ml; $P < 0.03$).

BAFF blockade with a single dose of adenovirus expressing either TACI-Ig or BAFF-R-Ig at 8 weeks of age prevented nephritis and prolonged survival. There was no difference in survival of mice treated with the 2 BAFF antagonists and mice treated for 2 weeks with CTLA-4Ig in addition to AdBAFF-R-Ig. All subsequent mechanistic studies were therefore performed on mice treated with a single dose of AdBAFF-R-Ig. BAFF-R-Ig levels attained by adenovirus injection ranged from 2 mg/ml to 6 mg/ml, as measured by BAFF-R–specific ELISA (12), in the first week after virus injection and decreased to undetectable levels by 6 weeks after injection (data not shown). As previously reported, treatment with AdCTLA-4Ig at 12 weeks of age did not prevent the onset of proteinuria in (NZW × BXSB) mice (5). In contrast, disease onset was delayed by a single dose of AdBAFF-R-Ig administered at 12 weeks of age, with a significant survival benefit in treated mice (Figure 1).

Despite the clear survival benefit, BAFF blockade did not prevent the emergence of either aCL or anti-Sm/RNP IgG autoantibodies. These autoantibodies appeared in the serum in equivalent

titers to those seen in controls by the age of 12–17 weeks (Figures 2A and B) and were predominantly of the IgG2a isotype, similar to those in control mice (data not shown). Furthermore, the range of binding affinities of aCL was similar in treated mice and controls (Figure 2C). However, significantly less renal histologic damage was observed at 22 and 32 weeks in the mice treated with AdBAFF-R-Ig than in age-matched controls (Figures 3A and C). There was also significantly less cardiac damage in mice treated with AdBAFF-R-Ig at 8 weeks of age than in untreated controls (Figures 3B and C).

In contrast to the protection against renal and cardiac damage afforded by BAFF blockade, there was less protection against the development of thrombocytopenia in treated mice. Platelet counts decreased significantly in both groups of AdBAFF-R-Ig–treated mice by the age of 17 weeks. Platelet counts were higher in AdBAFF-R-Ig–treated mice than in controls at 17 weeks but were not significantly different from those in controls by 22 weeks (Figure 3D).

Analysis of the mouse spleens revealed that there was a 50% decrease in the total number of spleen cells in 17-week-old AdBAFF-R-Ig–treated mice (Table 1). The percentage of B cells was also significantly decreased in treated mice. Analysis of B cell subsets showed that at 17 weeks, there was significant depletion of follicular B cells, with less effect on T1 and class-switched B cells (data not shown). Depletion of marginal zone B cells was also observed, although there are constitutively few of these cells in the (NZW × BXSB)F$_1$ strain. Partial recovery of B cells was observed by 22 weeks. The percentages of CD4 T cells and DCs were not changed in the spleens of treated mice (data not shown). However, as a result of the small spleen size, the total number of CD4 T cells and DCs per spleen was markedly decreased (Table 1). At 22 weeks, the spleens of treated mice were smaller than those of age-matched controls, and there were still significantly fewer activated B and T cells and fewer DCs than in age-matched untreated controls (Table 1). Similar results were observed in mice treated with AdTACI-Ig (data not shown).

B cell depletion was accompanied by a decrease in the total number of antibody-forming cells in the spleen, as evaluated by ELISpot assay at 17 weeks. Although the frequency of antibody-forming cells was not altered in the spleens of the treated mice, there was a 10-fold decrease in total IgM- and IgG-secreting cells in the spleens of mice treated at 8 weeks of age, and a 3–4–fold decrease in mice treated at 12 weeks of age. This was accompanied by a decrease in aPL-producing cells that was relatively less than the decrease in total antibody-forming cells. By 22 weeks, there was no longer any difference between treated and control mice in terms of the total number of antibody-forming cells in the spleen (Figure 2D). Similar results were observed in bone marrow, with a decrease in the frequency of aCL-forming cells in treated mice at 17 weeks that normalized by 22 weeks (data not shown).

We next examined the kidneys of 17- and 22-week-old treated mice and controls for deposition of immunoglobulin and for infiltration with inflammatory cells. Bright deposits of IgG were visible in the glomeruli in both control and treated mice at 17 weeks of age (Figures 4C and F). By 22 weeks of age, kidneys of control mice showed marked infiltration with inflammatory cells, especially F4/80-positive macrophages and CD11c-positive DCs. These cells were topologically segregated from each other. Macrophages were present throughout the interstitium and around the outside of glomeruli, whereas DCs were found within the glomerular tufts (Figures 4A and B). T cells were also scattered throughout the interstitium, and B cells accumulated in small lymphoid aggregates around blood vessels (results not shown). AdBAFF-R-Ig–treated mice had fewer inflammatory cells in the kidney than did controls, with very limited macrophage infiltration and less infiltration with DCs (Figures 4D and E). There were also fewer T and B cell infiltrates in the interstitium (data not shown). These findings were consistent with the results of the renal histologic analysis, which showed fewer interstitial infiltrates in treated mice (Figures 3A and C).

Because there was a lower inflammatory response to immune complex deposition in the glomeruli of treated mice than in control mice, we examined the expression of mediators of inflammation in the serum and kidneys. Anticardiolipin antibodies have been reported to induce endothelial expression of adhesion molecules, including E-selectin, P-selectin, ICAM, and VCAM, and this endothelial cell activation is thought to contribute to the thrombosis that occurs in APS (16,17). Kidneys from treated and control mice were therefore examined for expression of endothelial activation markers. Up-regulation of renal VCAM and P-selectin levels occurred in control mice older than 17 weeks with proteinuria. In contrast, 22–26–week old mice treated with AdBAFF-R-Ig or AdTACI-Ig at 8 weeks of age did not have increased expression of either molecule in the kidneys (Figures 5A and B). A similar trend was observed for the other adhesion molecules, but the differences did not reach statistical significance (data not shown).

Interestingly, 22-week-old mice that had been treated with AdBAFF-R-Ig at 12 weeks of age had elevated renal expression of VCAM, but not P-selectin, indicating only partial protection of the kidney. Serum levels of soluble VCAM increased in control mice by 15–17 weeks of age, even before the onset of proteinuria, but did not increase in mice treated with AdBAFF-R-Ig or AdTACI-Ig at 8 weeks of age. In contrast, mice treated with AdBAFF-R-Ig at 12 weeks of age had elevated serum levels of VCAM, consistent with the quantitative PCR data (Figure 5C). Serum levels of E-selectin did not differ between treated mice and controls (data not shown).

DISCUSSION

The $(NZW \times BXSB)F_1$ mouse is a model of 2 aspects of SLE: inflammatory renal disease and APS (3,5). Disease onset in these mice is T cell dependent and is prevented by depletion of T cells or by T cell costimulatory blockade before the age of 8 weeks (4,5). In contrast, once autoantibodies are present in the serum, the disease in $(NZW \times BXSB) F_1$ mice is refractory to treatment with the T cell costimulatory antagonist CTLA-4Ig, despite low numbers of activated T cells in the mice at this age, suggesting that disease perpetuation may be T cell independent (5). Similarly, APS in humans is refractory to conventional immunosuppression.

Disease in male $(NZW \times BXSB)F_1$ mice is accelerated by the *Yaa* gene, which increases the expression of TLR-7 by 2-fold (6). TLR-7 is expressed on plasmacytoid DCs and on B cells and is an innate sensor of single-stranded RNA, helping to protect against RNA viruses (18). Apoptotic blebs also contain RNA, and an excessive load of apoptotic material can break tolerance to this ubiquitous self antigen. Nucleic acid antigens can also be delivered to DCs by immune complexes in an Fc receptor–mediated manner and to B cells through the B cell receptor (8); these cells can then undergo TLR-7– mediated activation. The production of autoantibodies to RNP is completely dependent on TLR-7 (19,20). Cardiolipin is an antigenic component of apoptotic blebs (21); it is therefore possible that apoptotic blebs opsonized by aCL are taken up by plasmacytoid DCs and help break tolerance to nucleic acid antigens contained within the blebs (22). Apoptotic blebs may also be taken up directly by anticardiolipin B cells and activate them in a TLR-dependent manner, thus perpetuating the autoimmune response.

Plasmacytoid DCs activated through TLRs are a major source of type I interferons. Type I interferons activate myeloid DCs, resulting in the release of BAFF, a critical mediator of B cell survival and class switching (7,23). BAFF overexpression can rescue autoreactive B cells from anergy (24,25) and induces lupus-like disease in non–autoimmune-prone mice (26,27). This disease, which is associated with the production of class-switched IgG antibodies to DNA, deposition of immune complexes in the kidney, and GN, occurs even in the absence of T cells but is dependent on signaling through the TLR adaptor molecule myeloid differentiation factor

88 (9). Type I interferons also increase the sensitivity of B cells to TLR ligation (28), resulting in further amplification of the disease process. Thus, although disease onset in (NZW × BXSB) F_1 mice is T cell dependent, it is possible that once IgG autoantibody–producing B cells are present, immune complexes could perpetuate disease in a TLR- and BAFF-dependent manner. For this reason, we investigated whether BAFF blockade is an effective therapeutic approach for APS.

Our results showed that a short course of BAFF blockade effectively prevented both the thrombotic vasculopathy caused by aPL and the immune complex–mediated GN that occur in (NZW × BXSB)F_1 mice. In addition, when administration of BAFF blockade was delayed until after autoantibodies appeared in the serum, a significant survival benefit was still observed. This beneficial effect was achieved by selective blockade of BAFF alone, indicating that APRIL does not contribute to disease pathogenesis. However, BAFF blockade did not decrease the titers of IgG aCL and anti-Sm/RNP antibodies. Since both marginal zone B cells and extrafollicular antibody-forming B cells are highly sensitive to BAFF blockade (12), this suggests that antiphospholipid-producing B cells do not arise from either of these subsets. Furthermore, the relative affinities of aCL were similar in AdBAFF-R-Ig–treated and control mice.

These results are similar to those we and others have observed in (NZW × BXSB)F_1 mice, in which the formation of spontaneous germinal centers is resistant to BAFF blockade, and class-switched and somatically mutated anti–double-stranded DNA antibodies still arise after a short delay (11,12,29). These data are also consistent with findings in BAFF-deficient mice, in which germinal centers still form after immunization with a T cell–dependent antigen. Although these are smaller and are of shorter duration than those that arise in non–BAFF-deficient mice, affinity maturation remains intact (30). Finally, BAFF-deficient mice on an autoimmune genetic background can still produce high-titer autoantibodies (31).

Although affinity is not the only determinant of pathogenicity, our results further showed that at least some of the autoantibodies that arose after BAFF blockade had pathogenetic potential. Autoantibodies to platelets that arise in (NZW × BXSB)F_1 mice can rapidly transfer thrombocytopenia to wild-type controls due to Fc receptor–mediated clearance of coated platelets (32,33). In mice treated with BAFF blockade, the onset of thrombocytopenia was only modestly delayed, indicating that pathogenetic autoantibodies directed to platelets were generated and that Fc receptor–mediated clearance could still occur. In addition, analysis of the kidneys showed that autoantibodies were deposited in the glomeruli early in the disease course, consistent with the lack of effect of BAFF blockade on serum autoantibody titers. However, autoantibody deposition was dissociated from renal inflammatory disease in (NZW × BXSB)F_1 mice in the setting of BAFF deficiency.

BAFF blockade induced a marked depletion of B cells. The reduction in the total number of IgG anticardiolipin autoantibody–forming B cells in these mice (mean ± SD $4.4 \pm 2.1 \times 10^3$ cells per spleen in 17-week-old BAFF-R-Ig–treated mice versus $28.1 \pm 23.7 \times 10^3$ cells per spleen in control mice) did not, however, result in a proportional decrease in autoantibody titers. Since the affinity of the autoantibodies does not appear to be higher in treated mice than in controls, possible explanations for this include increased plasma cell lifespan after leaving the spleen, increased amount of antibody secretion per cell, or increased half-life of the serum immunoglobulin as a compensatory measure.

The beneficial effects of BAFF blockade observed in (NZW × BXSB)F_1 mice are most likely accounted for by the decrease in the number of B cells. B cells have many effector functions in the immune system, apart from their ability to secrete immunoglobulin (34). Autoreactive B cells take up autoantigen and can present it to T cells in a manner different from that of DCs;

this presentation of cryptic antigen can contribute to T cell activation and loss of T cell tolerance (35). In the context of autoimmunity, loss of B cells results in a decrease in autoantigen presentation to T cells (36) and decreased numbers of activated T cells, as observed in the present study. In addition, B cells secrete chemokines involved in splenic T cell accumulation, organization of T cell zones, and splenic DC development. Depletion of B cells, regardless of antigenic specificity, therefore results in a smaller spleen size and a decrease in the total number of T cells and DCs in the spleen (37). Finally, activated B cells secrete inflammatory cytokines and can migrate to sites of inflammation, where they may contribute to tissue-specific immune responses.

We propose that the decrease in T cells and in TLR-7–expressing B cells and DCs in treated mice resulted in a significantly decreased inflammatory burden that impacted both the inflammatory nephritis and the thrombotic tendency in the $(NZW \times BXSB)F_1$ mice. Even at 22 weeks of age, there were 4-fold fewer activated T and B cells and 3-fold fewer DCs in the spleens of treated mice than in controls. The degree of cellular infiltration into the kidneys of mice treated with preventive BAFF blockade was markedly decreased, and renal expression of multiple mediators of inflammation was not increased above that observed in young mice (Bethunaickan R: unpublished observations).

We have previously shown in a different model of SLE nephritis that the onset of proteinuria is associated with renal up-regulation of the expression of endothelial activation markers (15). In $(NZW \times BXSB)F_1$ mice, we found that despite the production of autoantibodies and their deposition in the kidneys, endothelial activation, as manifested by the release of soluble VCAM into the serum and production of VCAM and P-selectin in the kidney, was significantly delayed by early treatment with BAFF-R-Ig or TACI-Ig. These findings suggest that both autoantibodies and circulating mediators of inflammation contribute to endothelial activation in $(NZW \times BXSB)F_1$ mice.

In addition, inflammation is known to alter properties of proteins of the coagulation cascade. Inflammatory cytokines such as interleukin-1 and TNFα can down-regulate natural anticoagulants such as thrombo-modulin and endothelial protein C receptor. An inflammatory environment also enhances the production of procoagulants, such as tissue factor, and this in turn amplifies inflammatory pathways (38). Thus, a decreased inflammatory burden may protect against thrombosis by altering the coagulation cascade itself. Recovery of spleen numbers after a short course of BAFF blockade takes several months and most likely accounts for the longevity of the mice after BAFF blockade.

Little is currently known about the effects of B cell depletion in human APS, although there have been some anecdotal reports of excellent responses to rituximab, which in some cases, did not decrease the anticardiolipin response (39). It remains to be determined whether depletion of effector B cells will decrease the risk of thromboses in humans who still produce aCL.

Acknowledgements

References

1. Hanly JG. Antiphospholipid syndrome: an overview. CMAJ 2003;168:1675–82. [PubMed: 12821621]

2. Oyaizu N, Yasumizu R, Miyama-Inaba M, Nomura S, Yoshida H, Miyawaki S, et al. (NZW × BXSB) F1 mouse: a new animal model of idiopathic thrombocytopenic purpura. J Exp Med 1988;167:2017–22. [PubMed: 3290385]

3. Yoshida H, Fujiwara H, Fujiwara T, Ikehara S, Hamashima Y. Quantitative analysis of myocardial infarction in (NZW × BXSB)F1 hybrid mice with systemic lupus erythematosus and small coronary artery disease. Am J Pathol 1987;129:477–85. [PubMed: 3425688]

4. Adachi Y, Inaba M, Sugihara A, Koshiji M, Sugiura K, Amoh Y, et al. Effects of administration of monoclonal antibodies (anti-CD4 or anti-CD8) on the development of autoimmune diseases in (NZW × BXSB)F1 mice. Immunobiology 1998;198:451–64. [PubMed: 9562869]

5. Akkerman A, Huang W, Wang X, Ramanujam M, Schiffer L, Madaio M, et al. CTLA4Ig prevents initiation but not evolution of anti-phospholipid syndrome in NZW/BXSB mice. Autoimmunity 2004;37:445–51. [PubMed: 15621570]

6. Pisitkun P, Deane JA, Difilippantonio MJ, Tarasenko T, Satterthwaite AB, Bolland S. Autoreactive B cell responses to RNA-related antigens due to TLR7 gene duplication. Science 2006;312:1669–72. [PubMed: 16709748]

7. Jego G, Pascual V, Palucka AK, Banchereau J. Dendritic cells control B cell growth and differentiation. Curr Dir Autoimmun 2005;8:124–39. [PubMed: 15564719]

8. Marshak-Rothstein A, Rifkin IR. Immunologically active autoantigens: the role of Toll-like receptors in the development of chronic inflammatory disease. Annu Rev Immunol 2007;25:419–41. [PubMed: 17378763]

9. Groom JR, Fletcher CA, Walters SN, Grey ST, Watt SV, Sweet MJ, et al. BAFF and MyD88 signals promote a lupuslike disease independent of T cells. J Exp Med 2007;204:1959–71. [PubMed: 17664289]

10. Ramanujam M, Davidson A. The current status of targeting BAFF/BLyS for autoimmune diseases. Arthritis Res Ther 2004;6:197–202. [PubMed: 15380033]

11. Ramanujam M, Wang X, Huang W, Schiffer L, Grimaldi C, Akkerman A, et al. Mechanism of action of transmembrane activator and calcium modulator ligand interactor-Ig in murine systemic lupus erythematosus. J Immunol 2004;173:3524–34. [PubMed: 15322217]

12. Ramanujam M, Wang X, Huang W, Liu Z, Schiffer L, Tao H, et al. Similarities and differences between selective and nonselective BAFF blockade in murine SLE. J Clin Invest 2006;116:724–34. [PubMed: 16485042]

13. Mihara M, Tan I, Chuzhin Y, Reddy B, Budhai L, Holzer A, et al. CTLA4Ig inhibits T cell-dependent B-cell maturation in murine systemic lupus erythematosus. J Clin Invest 2000;106:91–101. [PubMed: 10880052]

14. Chan O, Madaio MP, Shlomchik MJ. The roles of B cells in MRL/lpr murine lupus. Ann N Y Acad Sci 1997;815:75–87. [PubMed: 9186641]

15. Schiffer L, Bethunaickan R, Ramanujam M, Huang W, Schiffer M, Tao H, et al. Activated renal macrophages are markers of disease onset and disease remission in lupus nephritis. J Immunol 2008;180:1938–47. [PubMed: 18209092]

16. Del Papa N, Guidali L, Spatola L, Bonara P, Borghi MO, Tincani A, et al. Relationship between anti-phospholipid and anti-endothelial cell antibodies III: β2 glycoprotein I mediates the antibody binding to endothelial membranes and induces the expression of adhesion molecules. Clin Exp Rheumatol 1995;13:179–85. [PubMed: 7544710]

17. Meroni PL, Raschi E, Camera M, Testoni C, Nicoletti F, Tincani A, et al. Endothelial activation by aPL: a potential pathogenetic mechanism for the clinical manifestations of the syndrome. J Autoimmun 2000;15:237–40. [PubMed: 10968917]

18. Yasuda K, Richez C, Maciaszek JW, Agrawal N, Akira S, Marshak-Rothstein A, et al. Murine dendritic cell type I IFN production induced by human IgG-RNA immune complexes is IFN regulatory factor (IRF)5 and IRF7 dependent and is required for IL-6 production. J Immunol 2007;178:6876–85. [PubMed: 17513736]

19. Christensen SR, Shupe J, Nickerson K, Kashgarian M, Flavell RA, Shlomchik MJ. Toll-like receptor 7 and TLR9 dictate autoantibody specificity and have opposing inflammatory and regulatory roles in a murine model of lupus. Immunity 2006;25:417–28. [PubMed: 16973389]

20. Berland R, Fernandez L, Kari E, Han JH, Lomakin I, Akira S, et al. Toll-like receptor 7-dependent loss of B cell tolerance in pathogenic autoantibody knockin mice. Immunity 2006;25:429–40. [PubMed: 16973388]

21. Sorice M, Circella A, Misasi R, Pittoni V, Garofalo T, Cirelli A, et al. Cardiolipin on the surface of apoptotic cells as a possible trigger for antiphospholipids antibodies. Clin Exp Immunol 2000;122:277–84. [PubMed: 11091286]

22. Cline AM, Radic MZ. Murine lupus autoantibodies identify distinct subsets of apoptotic bodies. Autoimmunity 2004;37:85–93. [PubMed: 15293878]

23. Baccala R, Hoebe K, Kono DH, Beutler B, Theofilopoulos AN. TLR-dependent and TLR-independent pathways of type I interferon induction in systemic autoimmunity. Nat Med 2007;13:543–51. [PubMed: 17479100]

24. Lesley R, Xu Y, Kalled SL, Hess DM, Schwab SR, Shu HB, et al. Reduced competitiveness of autoantigen-engaged B cells due to increased dependence on BAFF. Immunity 2004;20:441–53. [PubMed: 15084273]

25. Thien M, Phan TG, Gardam S, Amesbury M, Basten A, Mackay F, et al. Excess BAFF rescues self-reactive B cells from peripheral deletion and allows them to enter forbidden follicular and marginal zone niches. Immunity 2004;20:785–98. [PubMed: 15189742]

26. Mackay F, Woodcock SA, Lawton P, Ambrose C, Baetscher M, Schneider P, et al. Mice transgenic for BAFF develop lymphocytic disorders along with autoimmune manifestations. J Exp Med 1999;190:1697–710. [PubMed: 10587360]

27. Khare SD, Sarosi I, Xia XZ, McCabe S, Miner K, Solovyev I, et al. Severe B cell hyperplasia and autoimmune disease in TALL-1 transgenic mice. Proc Natl Acad Sci U S A 2000;97:3370–5. [PubMed: 10716715]

28. Lau CM, Broughton C, Tabor AS, Akira S, Flavell RA, Mamula MJ, et al. RNA-associated autoantigens activate B cells by combined B cell antigen receptor/Toll-like receptor 7 engagement. J Exp Med 2005;202:1171–7. [PubMed: 16260486]

29. Gross JA, Johnston J, Mudri S, Enselman R, Dillon SR, Madden K, et al. TACI and BCMA are receptors for a TNF homologue implicated in B-cell autoimmune disease. Nature 2000;404:995–9. [PubMed: 10801128]

30. Rahman ZS, Rao SP, Kalled SL, Manser T. Normal induction but attenuated progression of germinal center responses in BAFF and BAFF-R signaling-deficient mice. J Exp Med 2003;198:1157–69. [PubMed: 14557413]

31. Jacob CO, Pricop L, Putterman C, Koss MN, Liu Y, Kollaros M, et al. Paucity of clinical disease despite serological autoimmunity and kidney pathology in lupus-prone New Zealand mixed 2328 mice deficient in BAFF. J Immunol 2006;177:2671–80. [PubMed: 16888029]

32. Nimmerjahn F, Bruhns P, Horiuchi K, Ravetch JV. FcγRIV: a novel FcR with distinct IgG subclass specificity. Immunity 2005;23:41–51. [PubMed: 16039578]

33. Mizutani H, Engelman RW, Kurata Y, Ikehara S, Good RA. Development and characterization of monoclonal antiplatelet autoantibodies from autoimmune thrombocytopenic purpura-prone (NZW × BXSB)F1 mice. Blood 1993;82:837–44. [PubMed: 8338948]

34. Lipsky PE. Systemic lupus erythematosus: an autoimmune disease of B cell hyperactivity. Nat Immunol 2001;2:764–6. [PubMed: 11526379]

35. Bockenstedt LK, Gee RJ, Mamula MJ. Self-peptides in the initiation of lupus autoimmunity. J Immunol 1995;154:3516–24. [PubMed: 7534800]

36. Shlomchik MJ, Craft JE, Mamula MJ. From T to B and back again: positive feedback in systemic autoimmune disease. Nat Rev Immunol 2001;1:147–53. [PubMed: 11905822]

37. Ngo VN, Cornall RJ, Cyster JG. Splenic T zone development is B cell dependent. J Exp Med 2001;194:1649–60. [PubMed: 11733579]

38. Esmon CT. Inflammation and the activated protein C anticoagulant pathway. Semin Thromb Hemost 2006;32 Suppl 1:49–60. [PubMed: 16673266]

39. Erre GL, Pardini S, Faedda R, Passiu G. Effect of rituximab on clinical and laboratory features of antiphospholipid syndrome: a case report and a review of literature. Lupus 2008;17:50–5. [PubMed: 18089684]
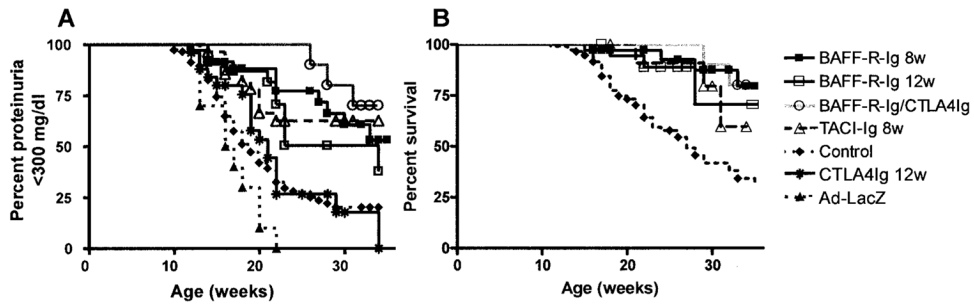
Figure 1.
Delay in the onset of proteinuria and mortality in $(NZW \times BXSB)F_1$ mice after BAFF blockade. **A,** Survival curves for onset of fixed proteinuria >300 mg/dl. Disease onset was significantly delayed in mice treated with AdBAFF-R-Ig at 8 weeks of age ($P < 0.001$), mice treated with AdBAFF-R-Ig at 12 weeks of age ($P < 0.004$), and mice treated with AdTACI-Ig at 8 weeks age, ($P < 0.001$) as compared with controls. The addition of 2 weeks of treatment with CTLA-4Ig to AdBAFF-R-Ig treatment at 8 weeks of age did not significantly improve outcome over treatment with AdBAFF-R-Ig alone. **B,** Mortality curves for the effective treatments shown in **A**. Mortality was significantly delayed in mice treated with AdBAFF-R-Ig at 8 weeks of age ($P < 0.0001$), mice treated with AdBAFF-R-Ig at 12 weeks of age ($P < 0.08$), and mice treated with AdTACI-Ig at 8 weeks of age ($P < 0.05$) as compared with controls.
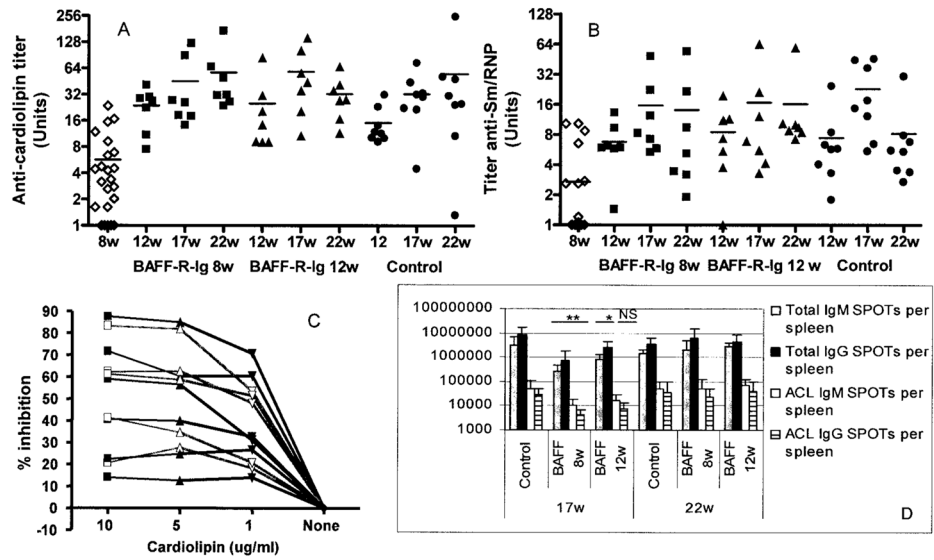
Figure 2.
BAFF blockade decreases the number of antibody-forming cells in the spleen but does not prevent the development of autoantibodies. **A** and **B,** Anticardiolipin (aCL) titers (**A**) and anti-Sm/RNP titers (**B**) for all 8-week-old mice, 12-, 17-, and 22-week-old mice treated at 8 weeks of age with AdBAFF-R-Ig, 12-, 17-, and 22-week-old mice treated at 12 weeks of age with AdBAFF-R-Ig, and 12-, 17-, and 22-week-old control mice. There was no difference in autoantibody titers between the treatment and control groups at any of the 3 ages. Horizontal bars show the mean. **C,** Inhibition curves for 6 serum samples from 17-week-old mice treated with AdBAFF-R-Ig at 8 weeks (gray lines) and 6 serum samples from 17-week-old control mice (black lines). Relative affinities were similar in the 2 groups. Each curve represents a single mouse. Values are the average of duplicate samples. **D,** Enzyme-linked immunospot (ELISpot) analysis of AdBAFF-R-Ig–treated mice and controls at 17 and 22 weeks of age. At 17 weeks of age, treated mice had significantly fewer IgM- and IgG-producing B cells in the spleen than did controls. Autoantibody-secreting B cells were decreased in mice treated at 8 weeks of age with AdBAFF-R-Ig. Values are the mean and SD. $* = P < 0.05$; $** = P < 0.02$ versus controls. NS = not significant.
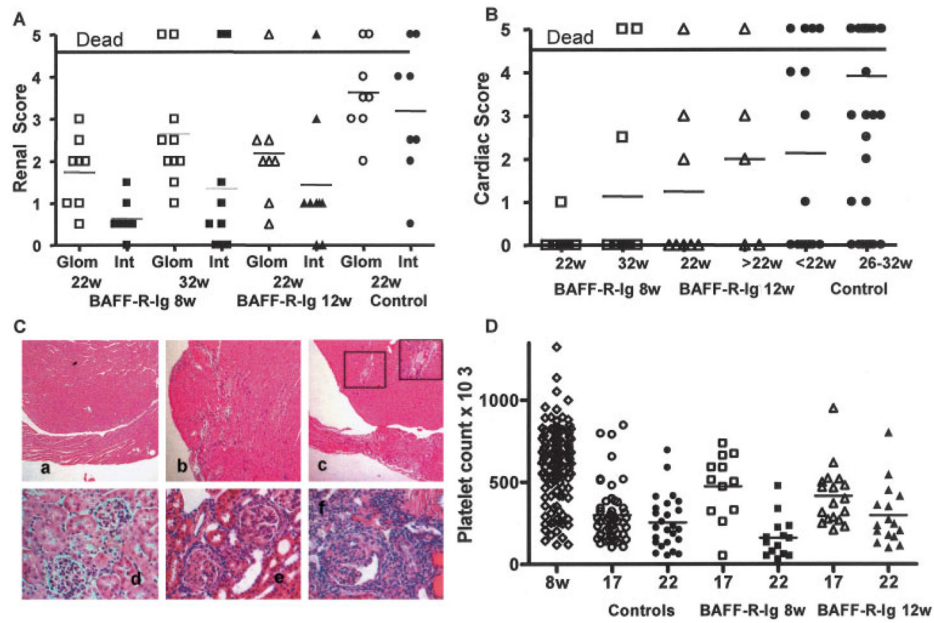
Figure 3.
AdBAFF-R-Ig protects against renal and cardiac damage, but not thrombocytopenia, in (NZW × BXSB)F$_1$ mice. **A** and **B,** Glomerular (Glom) and interstitial (Int) damage scores (**A**) and cardiac damage scores (**B**) in treated and control mice at the indicated ages. Symbols above the graphs represent mice that died with proteinuria >300 mg/dl before their organs could be harvested. These mice were given arbitrary glomerular and interstitial damage scores of 3 for statistical analysis and were excluded from the analysis of cardiac damage. Mice treated at 8 weeks of age with AdBAFF-R-Ig had significantly less renal damage at 22 weeks ($P < 0.002$ for each score) and at 32 weeks ($P < 0.02$ for each score) than did controls. Mice treated at 12 weeks of age with AdBAFF-R-Ig had significantly less renal damage at 22 weeks than did controls ($P < 0.005$ for the glomerular score and $P < 0.05$ for the interstitial score), and mice treated at 8 weeks of age with AdBAFF-R-Ig had significantly less cardiac damage than did age-matched controls ($P < 0.05$). **C,** Hematoxylin and eosin–stained sections of hearts (**a–c**) and kidneys (**d–f**) from 22-week-old mice treated with AdBAFF-R-Ig (**a** and **d**) and in untreated controls (**b, c, e,** and **f**). Grade 3 (**b**) and grade 4 (**c**) cardiac damage with small-vessel thrombosis (insets in **c**) was observed in untreated controls. Severe glomerulonephritis with interstitial infiltrates and tubular casts were seen in untreated mice (**e** and **f**), but not in mice treated with AdBAFF-R-Ig (**d**). (Original magnification × 10 in **a–c**; × 40 in **d–f**.) **D,** Platelet counts in individual mice over time. Platelet counts were lower in treated 17-week-old mice than in 8-week-old mice ($P < 0.03$ for mice treated at 8 weeks and $P < 0.002$ for mice treated at 12 weeks) but were higher than those in untreated controls ($P < 0.005$ for both treatment groups). By 22 weeks, there was no difference in platelet counts between the treated groups and controls. In **A, B,** and **D,** symbols show scores in individual mice; horizontal bars show the mean score.
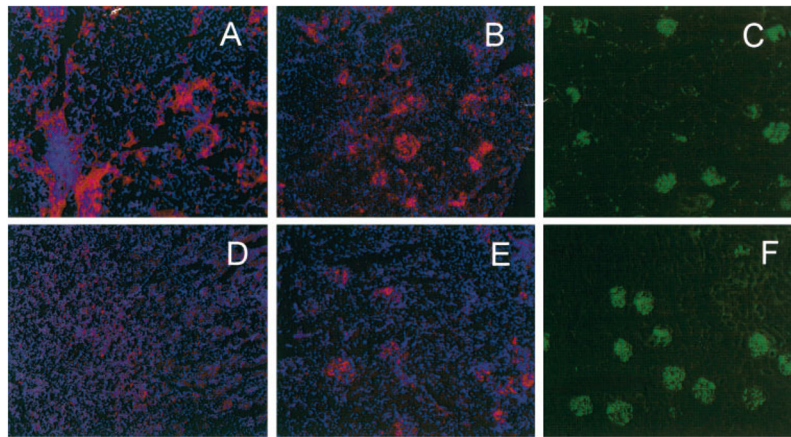
Figure 4.
Decreased renal infiltrates in the kidneys of treated mice. Samples from 22-week-old control mice (**A–C**) and 22-week-old mice treated at 8 weeks of age with AdBAFF–R–Ig (**D–F**) were stained with antibodies to F4/80 (**A** and **D**) and CD11c (**B** and **E**). Decreased infiltration with inflammatory cells was observed in treated mice. In control mice, F4/80-positive macrophage infiltration was observed in the interstitium and around glomeruli. CD11c-positive dendritic cell infiltration was observed within glomerular tufts. Equivalent deposition of IgG was observed in the glomeruli of control (**C**) and treated (**F**) mice. Results are representative of ≥5 mice per group. (Original magnification × 5.)
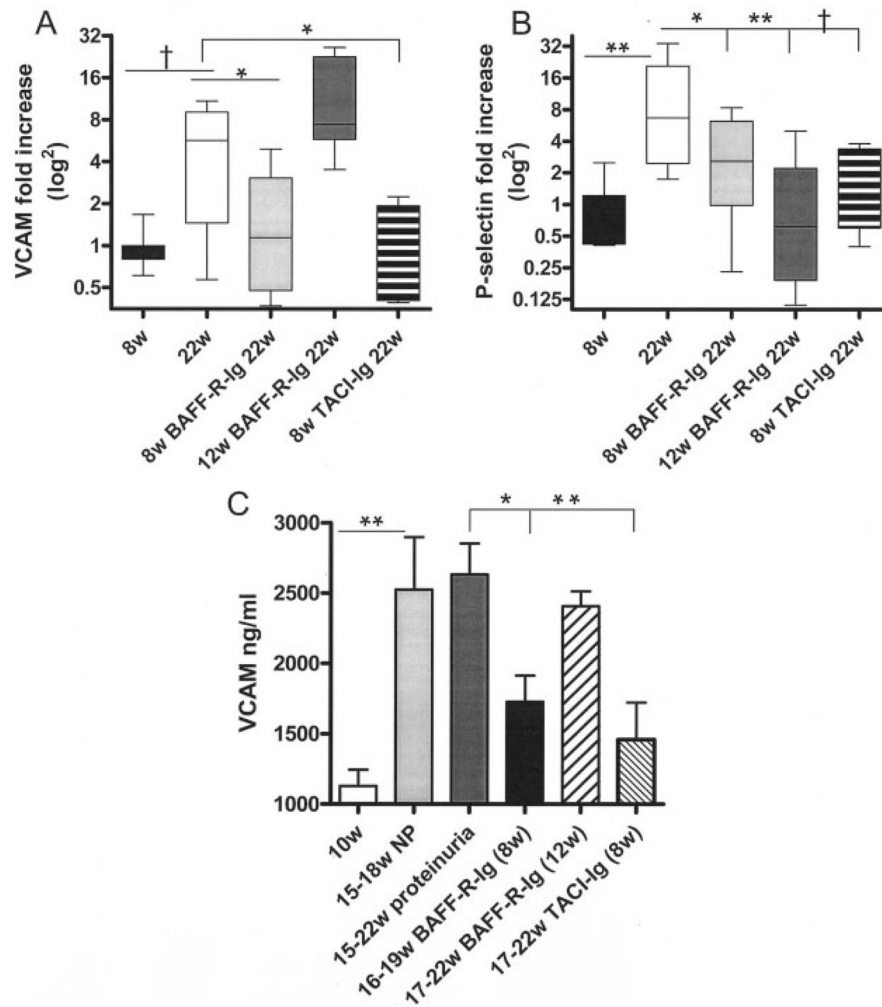
Figure 5.
Decreased expression of vascular cell adhesion molecule (VCAM) in the kidneys and serum of mice treated at 8 weeks of age with AdBAFF-R-Ig or AdTACI-Ig and of P-selectin in the kidneys of mice treated at 8 weeks of age or 12 weeks of age. **A** and **B,** Messenger RNA expression of VCAM (**A**) and P-selectin (**B**) in the kidneys of 8-week-old and 22-week-old control mice with proteinuria and in 22-week-old mice treated at 8 or 12 weeks of age with AdBAFF-R-Ig or treated at 8 weeks of age with TACI-Ig. Expression of VCAM was increased in the kidneys of mice with proteinuria and mice treated at 12 weeks of age, but not in age-matched mice treated with either TACI-Ig or AdBAFF-R-Ig at 8 weeks of age. Expression of P-selectin was increased in the kidneys of mice with proteinuria, but not in mice in any of the treatment groups. Data are presented as box plots, where the boxes represent the 25th to 75th percentiles, the lines within the boxes represent the mean, and whiskers represent the minimum and maximum range. **C,** Serum levels of VCAM in control and treated mice. Mice treated at 8 weeks of age with AdBAFF-R-Ig or AdTACI-Ig had significantly less circulating soluble VCAM than did age-matched controls. Bars show the mean and SD of 6–10 mice per group. ** = $P < 0.002$; † = $P < 0.01$; * = $P < 0.05$. NP = nonproteinuric.

Table 1

Absolute numbers of spleen cells in control mice and mice treated at 8 and 12 weeks with BAFF-R-Ig[*]

	17-week-old mice			22-week-old mice		
	Controls	Treated at age 8 weeks with BAFF-R-Ig	Treated at age 12 weeks with BAFF-R-Ig	Controls	Treated at age 8 weeks with BAFF-R-Ig	Treated at age 12 weeks with BAFF-R-Ig
Cell count, $\times 10^7$	32.7 ± 17.6	11.1 ± 6.5[†]	15.1 ± 4.4	97.3 ± 48.1	50.0 ± 83.8[‡][†]	27.1 ± 15.0[§]
CD4 T cells, $\times 10^7$	6.8 ± 4.1	2.3 ± 1.0	3.8 ± 0.9	17.8 ± 9.3	3.7 ± 3.8	3.5 ± 1.2
Activated, $\times 10^7$	2.0 ± 1.2	0.7 ± 0.5[¶]	0.9 ± 0.3	4.6 ± 2.8	1.0 ± 0.9[†]	1.3 ± 0.6[†]
Memory, $\times 10^7$	6.4 ± 3.8	1.8 ± 1.3[†]	2.5 ± 1.0	16.8 ± 9.3	3.6 ± 4.0[†]	2.6 ± 1.2[†]
Naïve, $\times 10^7$	0.4 ± 0.4	0.4 ± 0.2	0.8 ± 0.2	0.5 ± 0.3	0.1 ± 0.1[¶]	0.4 ± 0.3
CD8 T cells, $\times 10^7$	1.0 ± 0.6	1.5 ± 0.3	1.0 ± 0.5	3.0 ± 1.6	1.3 ± 0.4	0.8 ± 0.2
B cells, $\times 10^7$	14.9 ± 7.2	3.1 ± 2.4[§]	2.9 ± 1.8[†]	48.1 ± 27.4	15.4 ± 22.4	5.8 ± 2.6[¶]
Activated, $\times 10^7$	2.6 ± 1.6	0.6 ± 0.6[†]	0.5 ± 0.3	8.4 ± 5.1	2.2 ± 2.7[¶]	1.3 ± 0.7[¶]
Follicular, $\times 10^7$	9.9 ± 5.0	1.1 ± 1.1[§]	1.0 ± 0.9[†]	37.7 ± 21.2	ND	3.7 ± 1.7[¶]
Class-switched, $\times 10^6$	1.8 ± 1.3	0.5 ± 0.4[†]	0.7 ± 0.4	3.3 ± 2.1	ND	0.3 ± 0.2[¶]
Dendritic cells, $\times 10^6$	3.7 ± 2.8	1.0 ± 1.1	2.6 ± 1.7	14.1 ± 12.6	5.3 ± 10.2[¶]	4.1 ± 2.6[†]

[*] Values are the mean ± SD number of cells (n = 5–7 mice per group). ND = not determined.

[†] $P < 0.02$ versus age-matched controls.

[‡] This variability was accounted for by a single mouse (in a group of 6) with a very large spleen.

[§] $P < 0.002$ versus age-matched controls.

[¶] $P < 0.05$ versus age-matched controls.